Influence of the anodizing potential on the porosity of the anodic oxide film and on the corrosion resistance of AZ91D magnesium alloy

Mara Cristina Lopes de Oliveira[a], Viviam Serra Marques Pereira[b], Olandir Vercino Correa[c], Renato Altobelli Antunes[b,*]

[a]Electrocell Ind. Com. Equip. Elet. LTDA, Technology, Entrepreneurship and Innovation Center (CIETEC), 05508-000 São Paulo, SP, Brazil
[b]Engineering, Modeling and Applied Social Sciences Center (CECS), Federal University of ABC (UFABC), 09210-170 Santo André, SP, Brazil
[c]IPEN/CNEN-SP, Av. Prof. Lineu Prestes 2242, CEP 05508-900, São Paulo, SP, Brazil

* Corresponding author: Tel/Fax: 55 11 4996-8241
Email address: renato.antunes@ufabc.edu.br

Abstract

Die-cast AZ91D magnesium alloy specimens have been submitted to anodizing at different potentials. Anodizing was conducted in an environmental friendly solution comprised of 3 M KOH + 1 M Na_2SiO_3 at room temperature. The surface treatment was performed electrolytically at four different potentials: 3 V, 5 V, 8 V and 10 V. The corrosion resistance was evaluated by electrochemical impedance spectroscopy (EIS) and potentiodynamic polarization curves obtained after 7 days of immersion in a 3.5 wt.% NaCl solution at room temperature. The porosity of the anodic films was estimated by means of the linear polarization method. SEM images revealed that the surface oxide was more uniform for the anodic films obtained at 3 V and 5 V. The films obtained at these potentials were less porous than those formed at 8 V and 10 V, leading to a higher protective character.

Keywords: AZ91D; anodizing; porosity measurement; corrosion

1. Introduction

Magnesium alloys are highly recognized as potential candidates for engineering applications demanding lightweight structural materials such as in aerospace and automotive industries[1]. The AZ91 series which is alloyed with Al and Zn have been extensively used in the automotive sector[2]. Other attractive properties are electromagnetic shielding and intrinsic biocompatibility which expands the applicability of magnesium alloys to areas such as electronics and biomedical devices[3]. In spite of these valuable features, magnesium alloys have high chemical activity[4]. As a consequence, high corrosion susceptibility is frequently reported[5-7], which restricts the widespread application of these materials especially in aggressive environments[8].

Surface treatments are commonly employed to deal with this limitation. Gray and Luan[9] reviewed the corrosion protection treatments of magnesium alloys. Chemical conversion coatings, electrochemical and electroless plating, physical vapor deposition (PVD) coatings, laser surface alloying and hydride coatings are mentioned by the authors. Anodizing plays a prominent role among the surface treatments of magnesium

alloys. Its popularity arises from the typical adherent, thick, dense and abrasion-resistant character of the anodized layer[10]. The morphology and composition of the surface varies depending on the anodizing voltage and on the electrolyte in which the treatment is conducted[11]. The most important commercial anodizing processes are based on the use of environmental harmful inorganic compounds such as chromates and fluorides or toxic organics such as hexamethylenetetramine[12]. However, there is a strong research activity toward the development of environmentally friendly anodizing processes aiming at achieving high corrosion resistance without adding chromates and/or fluorides[13]. Fukuda et al.[14] proposed a new eco-friendly anodizing bath, consisting of only potassium hydroxide and sodium silicate. They observed that the anodic film formed on the surface of the AZ91D alloy was denser, thicker and more uniform when sodium was added to the bath. The anodic films were comprised of $Mg(OH)_2$ and few amounts of Mg_2SiO_4. The benefits of the presence of sodium silicate in the anodizing electrolyte to the corrosion resistance of the AZ91D alloy were also evidenced by Li et al.[15].

The importance of the anodizing potential to the quality of the anodic film formed on magnesium alloys was unequivocally showed by several authors[11,16]. Zhang et al.[16] have found that the corrosion resistance of anodized AZ91HP specimens was proportional to the anodizing voltage which influences both the thickness and morphology of the anodic film. Higher voltages promoted the formation of thicker and more porous anodic films. In this regard, the corrosive medium can diffuse more easily through anodized layers formed at higher potentials. The influence of porosity was assessed only qualitatively. Other reports have mentioned the relevance of porosity to the performance of anodized films on magnesium alloys[17,18]. However, a quantitative estimation of the porosity degree through the anodized layers by electrochemical methods is not found in the current literature.

In this context, we aimed at correlating the corrosion resistance of anodic films formed on the AZ91D magnesium alloy with the intrinsic porosity formed after anodizing in an environmentally friendly bath consisting of KOH with addition of Na_2SiO_3. The treatment was conducted at different voltages to investigate the influence of this parameter on the porosity of the anodized layers. The porosity of the anodic films was electrochemically determined using the linear polarization method. The corrosion resistance of the anodized specimens was evaluated by means of electrochemical impedance spectroscopy and potentiodynamic polarization curves. Scanning electron microscopy (SEM) was used to observe the morphology of the anodic films.

2. Experimental details

2.1 Material

Die-cast alloy AZ91D was used in this work. The nominal chemical composition of the alloy is given in Table 1.

Table 1. Nominal chemical composition of the AZ91D alloy.

Element	Al	Mn	Zn	Si	Fe	Cu	Ni	Mg
Mass (%)	8,30 – 9,70	0,15 mín.	0,35 – 1,00	0,10 máx.	0,005 máx.	0,030 máx.	0,002 máx.	Bal.

2.2 Anodizing process

The specimens were cut from the as-cast ingot in rectangular parts with approximately 1 cm^2. Next, the specimens were electrically connected to a copper wire and then embedded in room temperature curing epoxy resin. Before anodizing, the electrode surfaces were prepared by mechanical polishing with progressively finer SiC paper up to 1200 grit size.

The anodizing process was conducted in a 3 M KOH solution with addition of 1 M Na_2SiO_3 at room temperature. A three-electrode cell configuration was used for the treatment with the AZ91D as the working electrode, a standard calomel electrode (SCE) as reference and a platinum wire as the counter-electrode. The anodic films were produced at four different conditions of constant potentials: 3 V, 5 V, 8 V and 10 V. The potential was controlled with a potentiostat/galvanostat Autolab PGSTAT 100 which was used for all the electrochemical measurements performed in this work. The treatment was carried out for 1 h for each condition of potential.

2.3 Electrochemical measurements

2.3.1 Film porosity

Elsener et al.[19] proposed an electrochemical method to estimate the porosity of PVD layers based on the use of equation (1):

$$P = \left(\frac{R_{p,s}}{R_p} \right) x 10^{-|\Delta E_{corr}|/b_a} \qquad (1)$$

The porosity of the film is estimated from the change of the corrosion potential ($\Delta E_{corr} = E_{corr,substrate} - E_{corr,substrate+coating}$) caused by the presence of the coating layer and from individual measurements of the polarization resistance (R_p) of the bare and coated substrate. In equation (1) $R_{p,s}$ denotes the polarization resistance of the bare substrate and R_p is the polarization resistance of the coated substrate while b_a is the anodic Tafel slope of the bare substrate. $R_{p,s}$ and b_a are determined from separate measurements of the bare substrate. The values of R_p can be obtained by the linear polarization method which is valid only if the polarization current of the coating is negligible compared to that of the substrate and if the substrate does not passivated in the electrolyte[20]. We used this method to estimate the porosity degree of the anodized specimens of the AZ91D alloy. The measurements were conducted in a 3.5 wt.% NaCl solution at room temperature, right after stabilization of the open circuit potential.

2.3.2 Corrosion resistance

The corrosion resistance of the anodizing specimens was evaluated by means of electrochemical impedance spectroscopy (EIS) and potentiodynamic polarization curves. All the tests were carried out using a potentiostat/galvanostat Autolab PGSTAT 100 with a frequency response analyzer (FRA) module for the impedance measurements, using the same configuration described for the anodizing process. The EIS spectra were obtained over the frequency range of 100 kHz to 10 mHz, with acquisition of 10 points per decade, at the open circuit potential (OCP), with an

amplitude of the perturbation signal of 10 mV. Potentiodynamic polarization curves were obtained at a scanning rate of 1 $mV.s^{-1}$ from -0.5 V versus the OCP up to 0 V. The potentials mentioned in this work are referred to the standard calomel electrode. The tests were performed in a 3.5 wt.% NaCl solution at room temperature up to 7 days of immersion.

2.4 Scanning electron microscopy (SEM)

The surface morphology of the anodic films was observed by SEM, using a Leica/LEO 440i. A TM3000 Hitachi microscope was used to observe the morphology of specimens immersed in a NaCl 3.5 wt.% solution at room temperature, aiming to evaluate the corrosion degradation of the AZ91D alloy anodized at the conditions described in section 2.2.

3. Results and Discussion

3.1 Anodizing process

Chronoamperometric curves of the AZ91D anodized at different constant potentials are shown in Fig. 1. The anodic currents decrease with increasing voltages. The general behavior consisted of a steep current increase which is then followed by a current plateau after a specific anodization time that depended on the constant voltage applied during the treatment. For the samples anodized at 3 V and 5 V the plateau was reached after 1000 s while for those treated at 8 V and 10 V the steady state currents were observed after 400 s. It is noticeable that the currents during anodizing at 8 V and 10 V were more than ten times lower than those developed at 3 V and 5 V. This is clearly shown in Fig. 1b where the x-axis scale was expanded in order to facilitate the visualization of the small currents observed at 8 V and 10 V. According to Fukuda et al.[14] the anodic currents arise from both the anodic dissolution and formation of the anodic film. The initial increase of the current density observed in the chronoamperometric curves would be caused by the anodic dissolution of the magnesium alloy. The electric charge during anodizing was larger in the following order: 3 V > 5 V >> 8V > 10 V. This is an indication that the thicknesses of the anodic films follow the same order[21].

3.2 Surface morphology

The surface morphology of the AZ91D anodized at different constant voltages is shown in the SEM micrographs of Fig. 2. The images reveal that the anodic film on the surface of the samples anodized at 3 V and 5 V are relatively thick and porous whereas the films formed at 8 V and 10 V are smooth. This suggests that these films are also thinner than those formed at 3 V and 5 V, confirming the indications of the results obtained from the chronoamperometric curves. In fact, the samples anodized at 8 V and 10 V maintained a metallic lustre while those anodized at 3 V and 5 V showed a thicker anodic oxide and no metallic lustre after treatment. The metallic lustre of the samples anodized at 8 V and 10 V can be observed in the macroscopic images shown in Fig. 3. However, despite the thin character of the films formed at 8 V and 10 V small pores were clearly seen spreading throughout the whole surface of the samples as shown in Fig. 4.

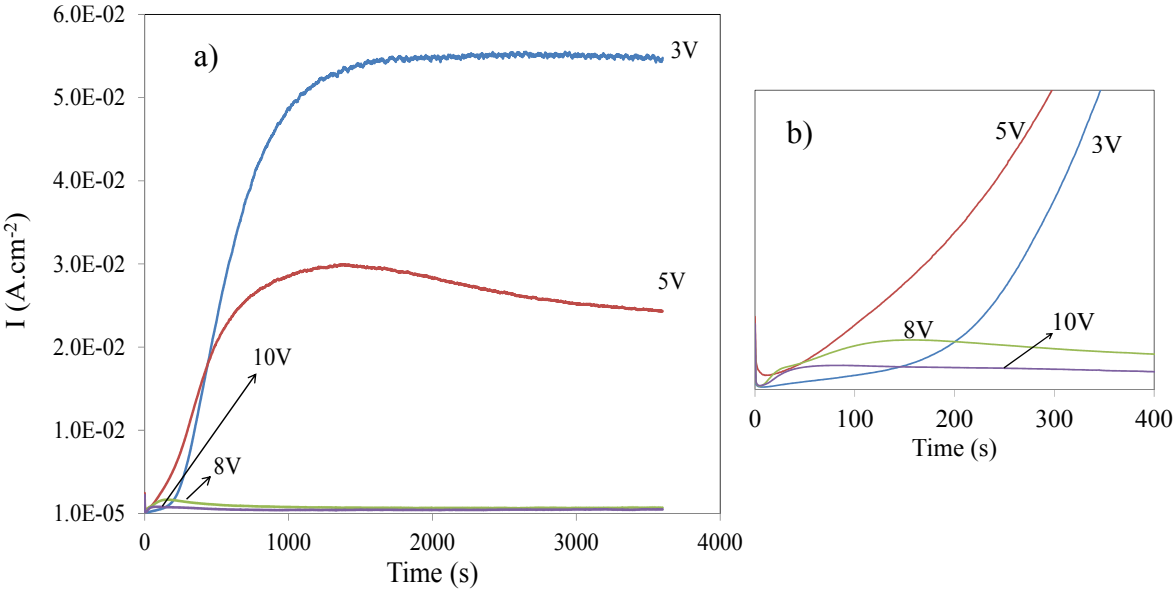

Figure 1. Chronoamperometric curves of the AZ91D alloy anodized at different constant voltages.

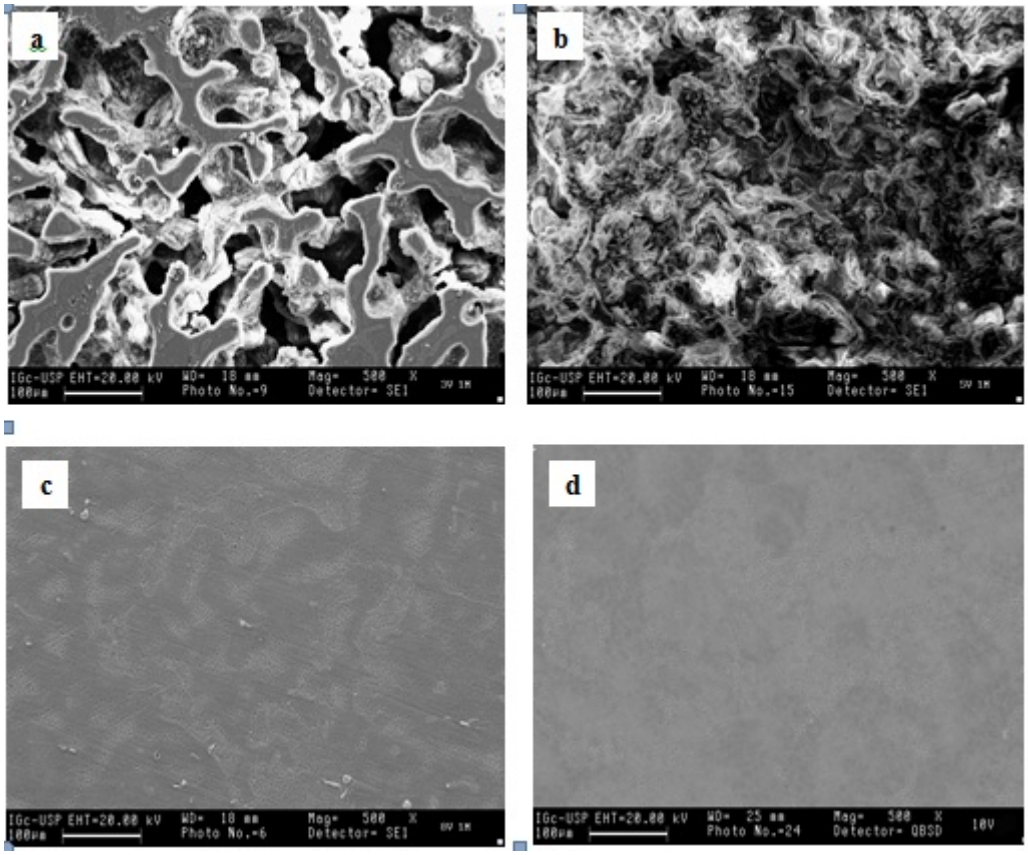

Figure 2. Surface morphology of the AZ91D alloy anodized at different constant voltages: a) 3 V; b) 5 V; c) 8 V and d) 10 V.

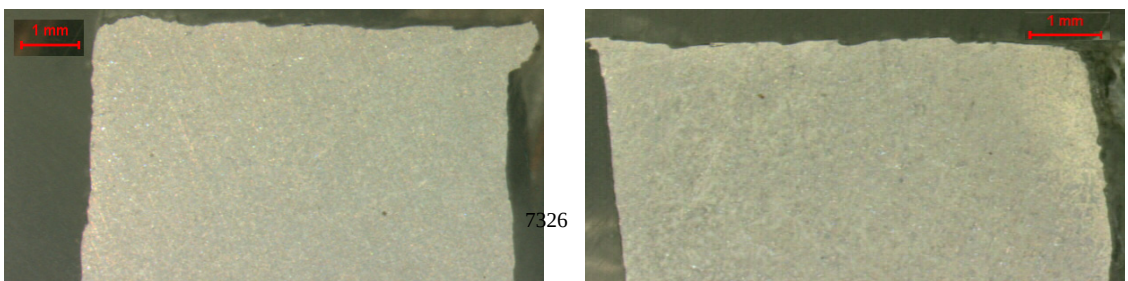

Figure 3. Optical micrographs of the samples anodized at: a) 8 V and b) 10 V.

3.3 Corrosion resistance

3.3.1 Electrochemical impedance spectroscopy (EIS)

Nyquist plots of the untreated and anodized AZ91D alloy obtained after 7 days of immersion in NaCl 3.5 wt.% solution at room temperature are shown in Fig. 5. Fig. 5a shows the plots for the untreated alloy and for the samples anodized at 5 V, 8 V and 10 V. The impedance values of the sample anodized at 3 V were significantly higher than those obtained for the other conditions. Thus, for clarity reasons, its plot is shown separately in Fig. 5b. For all the samples, the plots are characterized by a capacitive loop in the high frequency to medium frequency domain followed by an inductive behavior in the low frequency region. The inductive loop is less defined for the material anodized at 3 V as is clearly seen in Fig. 5b. The diameter of the Nyquist plot along the real axis is related to the charge transfer resistance (R_{ct}) of the electrode[22] which, in turn, indicates its corrosion resistance[23]. In this regard, the best anodizing condition that produced a significant increment of R_{ct} compared to the untreated alloy was for potential of 3 V. The sample anodized at 8 V presented the smallest diameter of the capacitive loop, denoting its poor protective character. The samples anodized at 5 V and 10 V were only marginally better than the untreated material.

The inductive loop at low frequencies is frequently reported for magnesium-based alloys[24,25]. According to Turhan et al.[22] inductive loops are associated with the dissolution of a metallic species yielding its cation to solution, involving an intermediate transition to an adsorbed species like the metal hydroxide. In the case of magnesium alloys, the presence of adsorbed $Mg()H)^{+}_{ads}$, $Mg(OH)_{2,ads}$ and Mg^{+}_{ads} would account for the inductive behavior in the low frequency domain of the Nyquist plots[26,27]. It is also reported that high concentrations of Mg ions on relatively film-free surfaces lead to the formation of inductive loops with high diameters[28]. As shown in Fig. 5, the inductive loop is only barely observed for the specimen anodized at 3 V (Fig. 5b). The presence of a protective oxide layer reduces the dissolution rate of the alloy. According to Anik and Celikten[29], the low-frequency inductive behavior tends to disappear in this case. In this regard, the anodizing process conducted at 3 V seems to be the most protective treatment employed in this work.

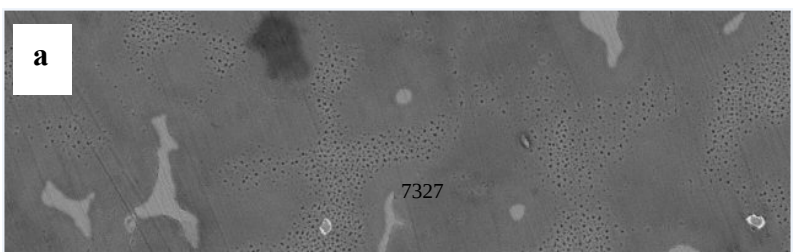

Figure 4. SEM micrographs of the samples anodized at: a) 8 V and b) 10 V, revealing the presence of small pores spreading throughout the anodized surfaces.

In order to give a visual indication of the relative chemical stability of the different anodized samples we performed immersion tests. The samples remained immersed during 7 days in NaCl 3.5 wt.% at room temperature, that is, the same conditions employed for the EIS measurements. Then, the top surfaces of the samples were observed using SEM. The images obtained before and after immersion are shown in Fig. 6. The non-anodized alloy was severely corroded. The samples anodized at 8 V and 10 V were completely covered by a thick surface oxide. The samples anodized at 5 V and 3 V were the least affected by the immersion conditions, confirming the higher protective character in comparison with those anodized at 8 V and 10 V.

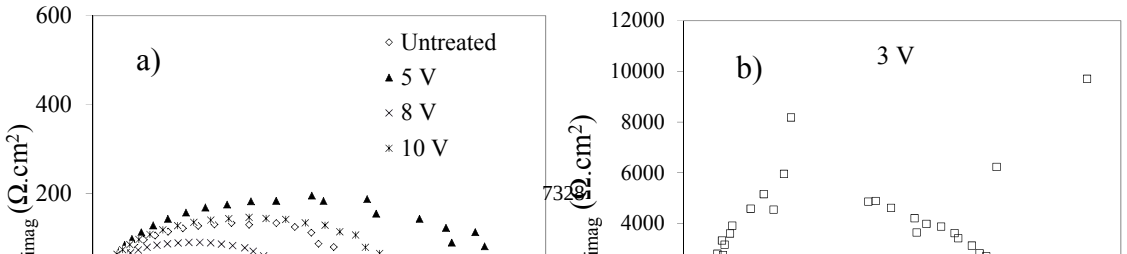

Figure 5. Nyquist plots of the untreated and anodized AZ91D alloy obtained after 7 days of immersion in NaCl 3.5 wt.% solution at room temperature.

3.3.2 Potentiodynamic polarization curves

Potentiodynamic polarization curves of the untreated and anodized AZ91D alloy obtained 7 days of immersion in NaCl 3.5 wt.% solution at room temperature are shown in Fig. 7. Table 2 shows the electrochemical data obtained from the polarization curves in Fig. 7. The corrosion current densities (I_{corr}) were determined using the Tafel's extrapolation method.
The samples anodized at 3 V and 5 V presented the lowest values of I_{corr} and the highest values of polarization resistance (R_p), indicating their superior corrosion resistance in comparison with the samples anodized at 8 V and 10 V. Moreover, the corrosion potential (E_{corr}) is also nobler for the samples anodized at 3 V and 5 V, confirming their higher stability during the measurements. It is noteworthy that the anodic Tafel's slope (b_a) was far higher for the anodized samples in comparison with the untreated alloy. This is an indication that the anodizing treatment, besides forming a physical barrier to the corrosive environment, restrains the anodic partial reaction, that is, magnesium oxidation, protecting the substrate. This is especially true for the anodizing conditions conducted at 3 V and 5 V. The cathodic Tafel's slope (b_c), in turn, was little affect by the anodizing treatment. These results support the findings from the EIS measurements.

3.4 Porosity determination

The results obtained from the linear polarization measurements for the untreated and anodized AZ91D alloy are shown in Tab. 3. The porosity of the anodic films was calculated according to equation (1). The results reveal that the samples anodized at 8 V and 10 V are less porous than those anodized 3 V and 5 V. This is in accordance with the visual aspect observed from the SEM micrographs shown in Figs. 2 and 5. According to Khaselev et al.[30] higher current densities during the anodizing process result in higher degree of porosity and more cracks in the anodized layers. The porosity levels shown in Table 2 agrees with the current densities achieved during the anodizing process as can be observed in the chronoamperometric curves shown in Fig. 1. It is noticeable that the corrosion resistance of the samples was inversely proportional to the porosity level shown in Table 3. The most protective anodized layers were obtained at 3 V and 5V as was unequivocally shown by the EIS measurements (Fig. 5) and potentiodynamic polarization curves (Fig. 7). Thus, it is clear that the corrosion resistance was determined rather by the thickness of the anodic film than for its porosity level.

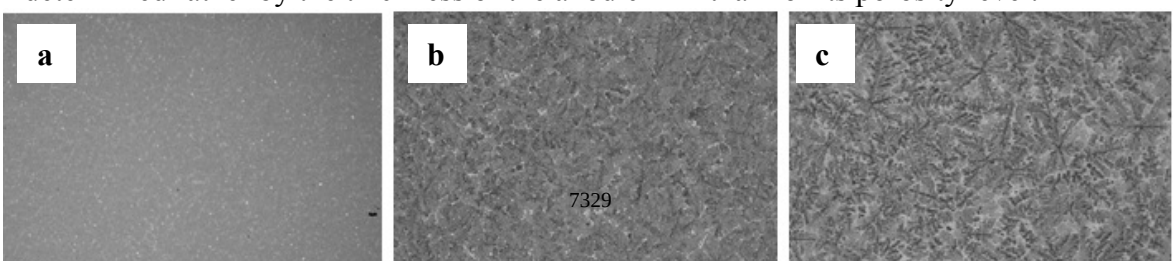

Figure 6. SEM micrographs of the untreated and anodized AZ91D samples, before immersion: a) untreated; b) 5 V; c) 3 V; g) 8 V; h) 10 V. The same samples after 7 days of immersion in NaCl 3.5 wt.% solution at room temperature: d) untreated; e) 5 V; f) 3 V; i) 8 V and j) 10 V.

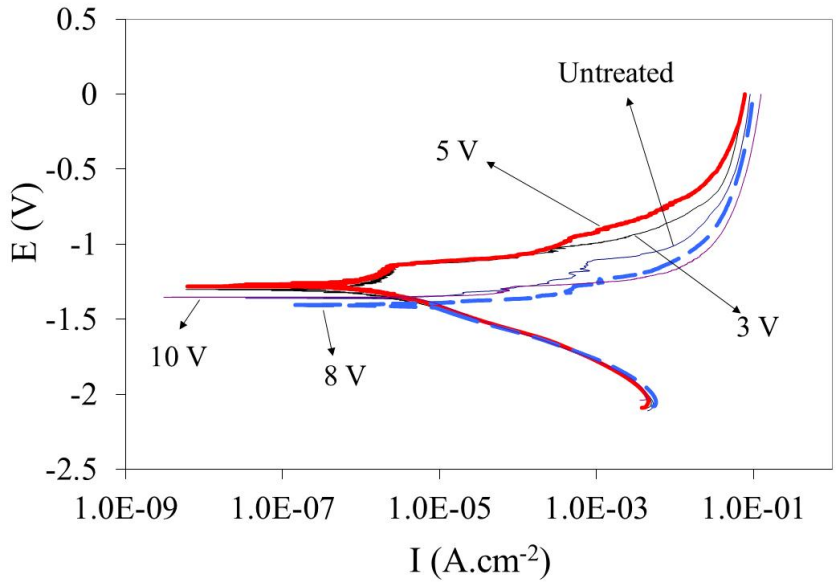

Figure 7. Potentiodynamic polarization curves of the untreated and anodized AZ91D alloy obtained 7 days of immersion in NaCl 3.5 wt.% solution at room temperature.

Table 2. Electrochemical data obtained from the potentiodynamic polarization curves in Fig. 7.

Sample	E_{corr} (V)	I_{corr} (μA.cm^{-2})	b_a (mV/decade)	b_c (mV/decade)	R_p (Ω.cm^2)
Untreated	-1.29	0.14	78	185	342
3 V	-1.26	0.54	590	182	8928
5 V	-1.28	0.26	483	167	9618
8 V	-1.40	1.25	160	51	248
10 V	-1.35	1.11	59	170	438

Table 3. Electrochemical parameters obtained from the linear polarization measurements and the calculated porosity of the AZ91D alloy anodized at different constant voltages.

Untreated AZ91D alloy				
$E_{corr,substrate}$ (mV)	$R_{p,s}$ (Ω.cm^2)	b_a mV/decade)		
-1609	940.8	42		
Anodized AZ91D alloy				
	3 V	5 V	8 V	10 V
$E_{corr,anodized}$ (mV)	-1586	-1592	-1600	-1596
R_p (Ω.cm^2)	410.2	617.4	1105	1048
Porosity (%)	65	60	52	44

4. Conclusions

The influence of the anodizing potential on the porosity level and on the corrosion resistance of the AZ91D magnesium alloy has been studied. The anodic films obtained at 3 V and 5 V were thicker than those obtained at 8 V and 10 V, as suggested by the chronoamperometric curves registered during the anodizing treatment. The metallic

lustre observed on the samples anodized at 8 V and 10 V confirms this indication. The anodizing potential strongly affected both the corrosion resistance and porosity of the anodic films. The corrosion resistance of the samples was higher for the anodizing potentials of 3 V and 5 V as well the porosity level of the anodic films. The corrosion resistance was rather determined by the thickness of the anodized layer than by its porosity level.

Acknowledgements

To Rima Industrial S/A for kindly providing the material used in this work.

References

1. Zuleta A.A., Correa E., Villada C., Sepúlveda M., Castaño J.G., Echeverría F. Comparative study of different environmentally friendly (Chromium-free) methods for surface modification of pure magnesium. *Surface & Coatings Technology*. 2011; 205: 5254-5259.
2. Ambat R., Aung N.N., Zhou W. Evaluation of microstructural effects on corrosion behavior of AZ91D magnesium alloy. *Corrosion Science*. 2000; 42: 1433-1455.
3. Zhang Y., Yan C. Development of anodic film on Mg alloy AZ91D. *Surface & Coatings Technology*. 2006; 201: 2381-2386.
4. Zhang S., Li Q., Yang X., Zhong X., Dai Y., Luo F. Corrosion resistance of AZ91D magnesium alloy with electroless plating pretreatment and Ni-TiO_2 composite coating. *Materiais Characterization*. 2010; 61: 269-276.
5. Alvarez-Lopez M., Pereda M.D., del Valle J.A., Fernandez-Lorenzo M., Garcia-Alonso M.C., Ruano O.A., Escudero M.I. Corrosion behaviour of AZ31 magnesium alloy with different grain sizes in simulated biological fluids. *Acta Biomaterialia*. 2010; 6: 1763-1771.
6. Abady G.M., Hilal N.H., El-Rabiee M., Badawy W.A. Effect of Al content on the corrosion behavior of Mg-Al alloys in aqueous solutions of different pH. *Electrochimica Acta*. 2010; 55: 6651-6658.
7. Uan J.-Y., Lin J.-K., Sun Y.-S., Yang W.-E., Chen L.-K., Huang H.-H. Surface coatings for improving the corrosion resistance and cell adhesion of AZ91D magnesium alloy through environmentally clean methods. *Thin Solid Films*. 2010; 518: 7563-7567.
8. Zhang Y., Yan C., Wang F., Lou H., Cao C. Study on the environmentally friendly anodizing of AZ91D magnesium alloy. *Surface & Coatings Technology*. 2002; 161: 36-43.
9. Gray J.E., Luan B. Protective coatings on magnesium and its alloys – a critical review. *Journal of Alloys and Compounds*. 2002; 336: 88-113.
10. Yabuki A., Sakai M. Anodic films formed on magnesium in organic, silicate-containing electrolytes. *Corrosion Science*. 2009; 51: 291-298.
11. Zhang R.F., Shan D.Y., Chen R.S., Han E.H. Effects of electric parameters on properties of anodic coatings formed on magnesium alloys. *Materials Chemistry and Physics*. 2008; 107: 356-363.
12. Blawert C., Dietzel W., Ghali E., Song G. Anodizing treatments for magnesium alloys and their effect on corrosion resistance in various environments. *Advanced Engineering Materials*. 2006; 8: 511-533.
13. Liu Y., Wei Z., Yang F., Zhang Z. Environmental friendly anodizing of AZ91D magnesium alloy in alkaline borate-benzoate electrolyte. *Journal of Alloys and Compounds*. 2011; 509: 6440-6446.

14. Fukuda H., Matsumoto Y. Effects of Na2SiO3 on anodization of Mg-Al-Zn alloy in 3 M KOH solution. *Corrosion Science*. 2004; 46: 2135-2142.
15. Li W., Zhu L., Liu H. Effects of silicate concentration on anodic films formed on AZ91D magnesium alloy in solution containing sílica sol. *Surface & Coatings Technology*. 2006; 201: 2505-2511.
16. Zhang S.-F., Hu G.-H, Zhang R.-F., Jia Z.-X., Wang L.-J., Wang Y.-J., Hu C.-Y., He X.-M. Effects of electric parameters on corrosion resistance of anodic coatings formed on magnesium alloys. *Transactions of Nonferrous Metals Society of China*. 2010; 20: s660-s664.
17. Wu C.S., Zhang Z., Cao F.H., Zhang L.J., Zhang J.Q., Cao C.N. Study on the anodizing of AZ31 magnesium alloys in alkaline borate solutions. *Applied Surface Science*. 2007; 253: 3893-3898.
18. Choi Y.-I., Salman S., Kuroda K., Okido M. Improvement in corrosion characteristics of AZ31 Mg alloy by square pulse anodizing between transpassive and active regions. *Corrosion Science*. 2012; 63: 5-11.
19. Elsener B., Rota A., Böhni H. Impedance study on the corrosion of PVD and CVD titanium nitride coatings *Materials Science Forum.* 1989; 44-45: 29-38.
20. Weng D., Jokiel P., Uebleis A., Boehni H. Corrosion and protection characteristics of zinc and manganese phosphate coatings. *Surface & Coatings Technology.* 1996; 88: 147-156.
21. Hiromoto S., Shishido T., Yamamato A., Maruyama N., Somekawa H., Mukai T. Precipitation control of calcium phosphate on pure magnesium by anodization. *Corrosion Science*. 2008; 50: 2906-2913.
22. Turhan M.C., Lynch R., Killian M.S., Virtanen S. Effect of acidic etching and fluoride treatment on corrosion performance in Mg alloy AZ91D (MgAlZn). *Electrochimica Acta.*. 2009; 55: 250-257.
23. Hsiao H.-Y., Tsai W.-T. Characterization of anodic films forme don AZ91D magnesium alloy. *Surface & Coatings Technology*. 2005; 190: 299-308.
24. Zhao M., Wu S., An P., Luo J. Study on the deterioration process of a chromium-free conversion coating on AZ91D magnesium alloy in NaCl solution. *Applied Surface Science*. 2006; 253: 468-475.
25. Jamesh M., Kumar S., Narayanan T.S.N.S. Corrosion behavior of commercially pure Mg and ZM21 Mg alloy in Ringer's solution – Long term evaluation by EIS. *Corrosion Science*. 2011; 53: 645-654.
26. Song G., Atrens A., Wu X., Zhang B. Corrosion behaviour of AZ21, AZ501 and AZ91 in solium chloride. *Corrosion Science*. 1998; 40: 1769-1791.
27. Baril G., Pébère N. The corrosion of pure magnesium in aerated and dearated sodium sulphate solutions. *Corrosion Science*. 2001; 43: 471-484.
28. Chen J., Wang J., Han E., Dong J., Ke W. AC impedance spectroscopy study of the corrosion behavior of an AZ91 magnesium alloy in 0.1 M solium sulfate solution. *Electrochimica Acta*. 2007; 52: 3299-3309.
29. Anik M., Celikten G. Analysis of the electrochemical reaction behavior of alloy AZ91 by EIS technique in H_3PO_4/KOH buffered K_2SO_4 solutions. *Corrosion Science*. 2007; 49: 1878-1894.
30. Khaselev O., Weiss D., Yahalom J. Structure and composition of anodic films formed on binary Mg-Al alloys in KOH-aluminate solutions under continuous sparking. *Corrosion Science*. 2001; 43: 1295-1307.